Rydberg Molecule-Induced Remote Spin Flips

Thomas Niederprüm,[1] Oliver Thomas,[1,2] Tanita Eichert,[1] and Herwig Ott[1,*]
[1]Research Center OPTIMAS, Technische Universität Kaiserslautern, 67663 Kaiserslautern, Germany
[2]Graduate School Materials Science in Mainz, Staudinger Weg 9, 55128 Mainz, Germany
(Received 22 April 2016; published 16 September 2016)

We have performed high resolution photoassociation spectroscopy of rubidium ultralong-range Rydberg molecules in the vicinity of the $25P$ state. Because of the hyperfine interaction in the ground state perturber atom, the emerging mixed singlet-triplet potentials contain contributions from both hyperfine states. We show that this can be used to induce remote spin flips in the perturber atom upon excitation of a Rydberg molecule. Furthermore, when the spin-orbit splitting of the Rydberg state is comparable to the hyperfine splitting in the ground state, the orbital angular momentum of the Rydberg electron is entangled with the nuclear spin of the perturber atom. Our results open new possibilities for the implementation of spin-dependent interactions for ultracold atoms in bulk systems and in optical lattices.

DOI: 10.1103/PhysRevLett.117.123002

Implementing tunable short-range interactions in ultracold quantum gases has proven to be key to study quantum phase transitions [1] and strongly interacting many-body systems [2,3]. The most commonly used techniques are magnetic Feshbach resonances [4] and confinement-induced effective interactions [5,6]. Long-range interactions beyond the pure contact interaction are more challenging to achieve. Possible realizations include second order tunneling [7], cavity-mediated interactions [8], magnetic dipolar interactions in high spin atomic species [9–11] and electric dipolar interactions between heteronuclear molecules [12]. Exciting atoms to Rydberg states is another way to induce long-range interactions, as evidenced by the demonstration of the Rydberg blockade [13–16] and antiblockade [17,18]. Recently, these concepts were transferred to the realm of ultracold quantum gases [19]. First experimental results with off-resonant excitation schemes show that for short times, coherent interactions between ground state atoms can be generated [20]. In most such "Rydberg dressing" schemes, the interaction is based on admixing Rydberg excitations to two particles, resulting in energy shifts which scale quadratically with the driving laser intensity. This narrows the parameter window for coherent effects drastically [20,21].

The discovery of Rydberg macrodimers [22,23] and Rydberg molecules [24] has opened up an increasing field of research, combining ultracold chemistry with many-body physics and low energy electron scattering. Rydberg molecules are bound by the contact interaction between the Rydberg electron and a ground state perturber atom. The large extension of the Rydberg electron wave function (50–1000 nm) makes it possible to induce long-range interactions between two spatially separated (remote) ground state atoms that, otherwise, interact solely through contact interaction on a typical length scale of 5 nm in the case of rubidium. In contrast to the usual Rydberg dressing of single species gases [21], only one excitation is required, thus, leading to a more favorable first order process, which scales linearly with the laser intensity.

For alkali atoms, one can distinguish three different types of molecules: ultralong range Rydberg molecules [24,25], trilobite molecules [26], and butterfly molecules [27–29]. While sharing a similar binding mechanism, they differ in the degree of perturbation, which is imposed by the ground state perturber to the Rydberg electron wave function. Here, we change the perspective and study the effect of the binding mechanism on the perturber atom. In agreement with theoretical predictions, we experimentally confirm the presence of spin-flip processes in the ground state perturber upon excitation of ultralong-range Rydberg molecules. We can also excite particular Rydberg states, where the Rydberg orbital angular momentum is strongly entangled with the nuclear spin of the perturber atom. For the $25P$ state of rubidium, both effects are active over a distance of up to 50 nm between the two atoms. As we use a single photon excitation scheme to excite the molecules, we avoid spontaneous scattering from an intermediate level. Our technique is, therefore, suited to induce coherent and dissipative interactions in ultracold atomic gases. This includes the realization of optical Feshbach resonances [30] involving Rydberg molecules and spin-dependent dissipative processes.

Based on Fermi's original idea of s-wave scattering by a quasifree electron [31], the interaction of a ground state perturber atom at a distance R inside the Rydberg wave function is described by a zero range pseudopotential $V_s(R) = 2\pi A_s(k_R)\delta(r-R)$ with a scattering length A_s that depends on the classical electron momentum $k_R = \sqrt{2/r - 1/n_{\mathrm{eff}}^2}$. Because of shape resonances appearing in the low energy scattering of electrons and alkali atoms, it is crucial to extend the pseudopotential to also include the p-wave scattering process [32]. Taking further into account the different scattering length for singlet and triplet scattering and the hyperfine structure in the perturber

atom, the Hamiltonian for the molecular system in Born-Oppenheimer approximation reads [33]

$$\hat{H} = \hat{H}_0 + 2\pi[a_s^S(k_R)\hat{\mathbb{I}}^S + a_s^T(k_R)\hat{\mathbb{I}}^T]\delta^{(3)}(\vec{r}-\vec{R}) + 6\pi[a_p^S(k_R)\hat{\mathbb{I}}^S + a_p^T(k_R)\hat{\mathbb{I}}^T]\delta^{(3)}(\vec{r}-\vec{R})\frac{\overleftarrow{\nabla}\cdot\vec{\nabla}}{k_R^2} + A\hat{\vec{S}}_2\cdot\hat{\vec{I}}_2. \quad (1)$$

Here, $\hat{H}_0$ is the atomic Hamiltonian of the Rydberg atom including the fine structure, a_s^S (a_s^T) are the s-wave scattering lengths for singlet (triplet) scattering, and a_p^S (a_p^T) are the p-wave scattering lengths for singlet (triplet) scattering. The projector on the triplet subspace can be expressed in terms of the spin $\hat{\vec{S}}_1$ of the Rydberg electron and the spin $\hat{\vec{S}}_2$ of the perturber and is given by $\hat{\mathbb{I}}^T = \hat{\vec{S}}_1\cdot\hat{\vec{S}}_2 + 3/4$. The singlet projector is $\hat{\mathbb{I}}^S = 1 - \hat{\mathbb{I}}^T$. The hyperfine coupling in the perturber is described by the hyperfine constant $A = 3.4$ GHz (for ^{87}Rb) and the coupling between the electronic spin $\hat{\vec{S}}_2$ and the nuclear spin $\hat{\vec{I}}_2$ of the perturber. Figure 1 shows the different angular momentum couplings that occur in the Rydberg molecules.

In order to calculate the Born-Oppenheimer potential energy curves (PECs), we have carried out a full diagonalization of the Hamiltonian (1), and the resulting eigenenergies, as a function of the internuclear distance R, are shown in Fig. 2(a). The corresponding excitation scheme, including the initial state of the two atoms, is shown in Fig. 1(c). As a consequence of the hyperfine interaction in the perturber atom, the singlet and triplet states are mixed and the Hilbert space can no longer be separated into the according subspaces. The emerging eigenenergies, therefore, feature one pure triplet potential energy curve [blue lines in Fig. 2(a)] and one of mixed singlet-triplet character (orange lines) [33–35]. This argument also applies the other way around: because of the singlet and triplet terms in the Hamiltonian, the subspaces of the $F = 1$ and the $F = 2$ hyperfine states of the perturber are mixed, and thus, the mixed character PEC contains both hyperfine states. The degree of hyperfine mixing depends on the relative strength of the Rydberg-ground state interaction with respect to the hyperfine interaction, and accordingly, we can identify two different regimes. In the more general case, which we denote as the spin-flip regime, the interaction is small compared to the hyperfine splitting, and thus, the admixture of the opposite hyperfine state is small. In the system at hand, this situation is realized for the $25P_{3/2}$, $F = 2$ and the $25P_{1/2}$, $F = 1$ states. For the latter, the molecular states have the form

$$|\Phi\rangle_{\mathrm{sf}} = \alpha|25P_{1/2}\rangle|F=1\rangle + \epsilon|25P_{1/2}\rangle|F=2\rangle + \cdots, \quad (2)$$

with $\alpha \approx 1$ and $\epsilon \ll 1$. The contribution of other states is of similar magnitude. Starting from two atoms in the $F = 2$ state, the small admixtures ϵ allow for the coupling to Rydberg molecules of opposite ground state spin and the excitation process can be seen as a spin-flip collision between the Rydberg electron and the ground state perturber. Since the created molecule is predominantly in the flipped spin state, the perturber atom will most likely pertain its flipped spin state, even upon spontaneous decay of the molecular state.

A peculiar second regime appears for the asymptotic free $25P_{1/2}$, $F = 2$ and $25P_{3/2}$, $F = 1$ states. Since the spin-orbit splitting of the $25P$ state almost equals the hyperfine splitting of the perturber, these two levels are separated by only 929 MHz, which is comparable to the Rydberg-ground state interaction energy at small internuclear distances. Consequently, the theory predicts strong mixing of up to 50% of the two states. For large internuclear distances, we still find an admixture of a few percent, even in the outermost well [Fig. 2(a)]. These states are predominantly a superposition of the two asymptotic ones,

$$|\Phi\rangle_{\mathrm{ent}} = a|25P_{1/2}\rangle|F=2\rangle + b|25P_{3/2}\rangle|F=1\rangle, \quad (3)$$

with $a, b \approx 0.1$–0.8, which entangle the fine structure state of the Rydberg atom with the hyperfine state of the perturber. They are distinct from the spin-flip regime by the much stronger mixing. We denote this regime as the "entanglement" regime.

In order to experimentally prove the existence of hyperfine mixing in Rydberg molecules, we photoassociate

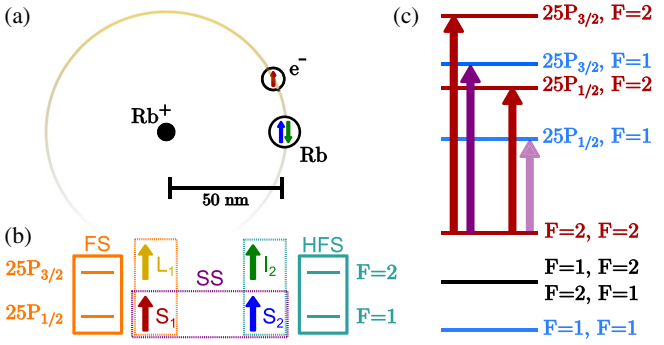

FIG. 1. (a) The contact interaction between the Rydberg electron e^- and the ground state atom Rb leads to a spin-dependent interaction over distances up to 50 nm in the $25P$ state. (b) The angular momentum coupling scheme shows how the spin-spin interaction (SS) couples the fine structure (FS) of the Rydberg atom with the hyperfine structure (HFS) of the perturber. The color of the arrows corresponds to the colors used in (a). (c) Transition scheme. When the sample is in the $F = 2$ ground state, only the atomic transitions to states adiabatically connecting to $F = 2$ states are possible (red arrows). Because of the hyperfine mixing of the molecular interaction (see text), transitions to molecular states in the $F = 1$ spectrum are also possible (purple arrows).

ultralong-range Rydberg molecules in the vicinity of the $25P$ state from a Bose-Einstein condensate (BEC) of ^{87}Rb. The experimental apparatus is described in detail in Ref. [36]. In brief, a BEC of 10^5 atoms and a temperature of 100 nK is prepared in a crossed optical dipole trap (1064 nm) by evaporation to final trapping frequencies of $2\pi \times 67$ Hz in all three directions. Because of a small magnetic field gradient present during evaporation, the BEC is spin polarized in the $5S_{1/2}$, $F = 1$, $m_F = +1$ ground state. Using microwave radiation, the spin state of the atoms can be transferred to the fully stretched $F = 2$, $m_F = +2$ state with a Landau-Zener sweep at a fidelity of close to 100%. The photoassociation of Rydberg molecules is achieved by a frequency doubled cw dye laser at a wavelength of 297 nm and a laser linewidth below 700 kHz. Once produced, the Rydberg molecules can decay into ions either by photoionization, leading to a Rb^+ atomic ion, or by associative ionization, leading to a Rb_2^+ molecular ion [37,38]. The experimental sequence consists of 1000 excitation pulses (1 μs) with subsequent continuous ion detection (200 μs). Because of the different mass, the atomic and molecular ions have a different TOF to the ion detector. From the decay of the signal, we can additionally extract the lifetime of the produced molecules. We have performed photoassociation spectroscopy with a resolution of 1 MHz, spanning more than 10 GHz.

The full spectrum for a BEC in the $F = 2$ state is shown in Fig. 2(b) along with the relevant parts of the spectrum for a BEC in the $F = 1$ state in Fig. 2(c). The most prominent features in each spectrum are the two bare atomic transitions, which can only appear for those states that match the hyperfine state of the prepared BEC. As discussed above, this no longer holds for the molecular states. Instead, some of the molecular lines of the $25P_{3/2}$, $F = 1$ spectrum also appear on the blue side of the $25P_{1/2}$, $F = 2$ state in the $F = 2$ spectrum [Fig. 2(d)]. As those lines can only originate from the mixed type potential, we compare, in Fig. 3, the lines in the $F = 2$ spectrum to the calculated energies of the lowest bound states in each well of the mixed type potential adiabatically connecting to the $25P_{3/2}$, $F = 1$ state (green bars). The three highest energy lines can not be attributed to a ground state in any of the wells and are probably higher

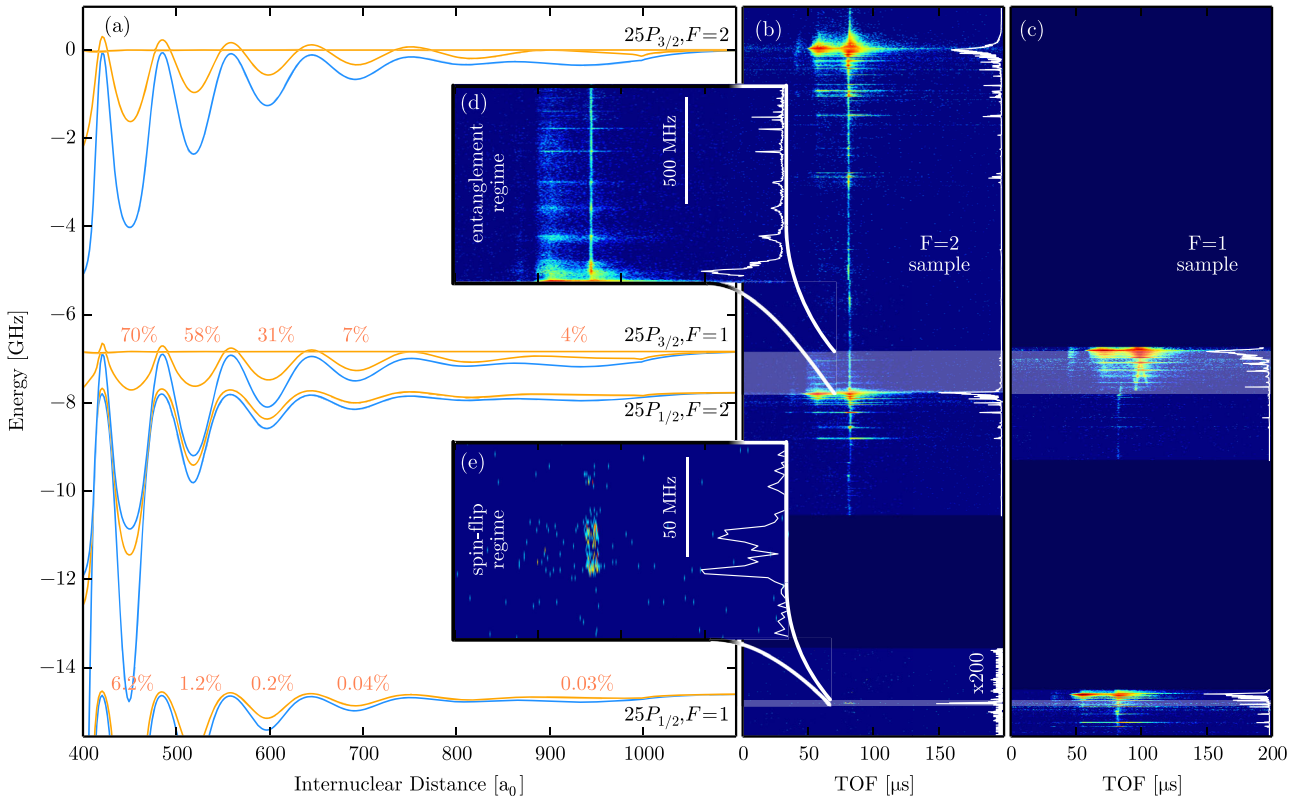

FIG. 2. (a) Adiabatic PECs for ultralong-range Rydberg molecules of rubidium 87. The PECs adiabatically connect to the four different $25P$ states. The blue PECs are of pure triplet type and do not mix the hyperfine states, the orange PECs are of mixed singlet-triplet character and contain both hyperfine states. The red numbers give the admixture of opposite spin to the states in the respective wells of the potential. (b) and (c) show the measured TOF spectrum for a BEC prepared in a pure $F = 2$ and $F = 1$ state, respectively. The energy scale coincides with the one of (a). The time of flight is 58 μs for the Rb^+ ions and 82 μs for the Rb_2^+. The deep blue regions were not measured. The white lines show the flight-time integrated spectrum. The insets (d) and (e) show zoom ins on highlighted parts of the $F = 2$ spectrum, illustrating the entanglement and the spin-flip regime, respectively. The employed TOF measurement technique allows us to extract the lifetime of the observed molecular resonances to an accuracy of 1 μs by fitting the temporal decay of the signal with an exponential function.

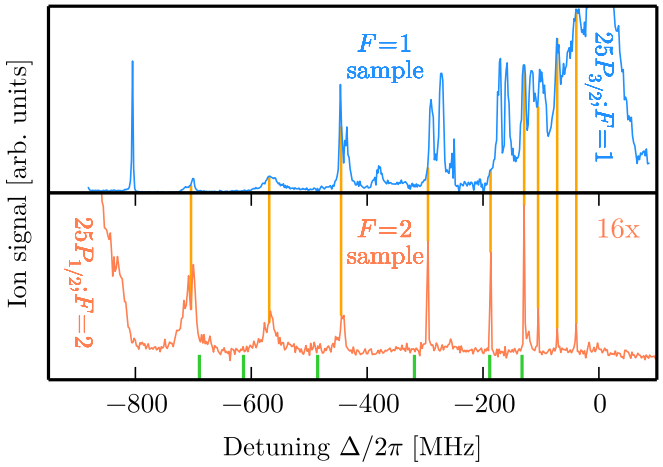

FIG. 3. Comparison of the molecular spectra in the region between the $25P_{3/2}$, $F = 1$ state (0 MHz) and the $25P_{1/2}$, $F = 2$ state (−929 MHz) in a sample with all atoms in the $F = 1$ state (blue) and all atoms in the $F = 2$ state (red). Since, in the $F = 2$ spectrum, we only observe the mixed type PEC (see text) that also appears in the $F = 1$ spectrum, every line in the $F = 2$ spectrum has a corresponding line in the $F = 1$ spectrum (orange lines). The calculated energies of the lowest bound states in each well of the mixed type PEC (green bars) agree with the observed resonances. Compared to the $F = 1$ spectrum, the $F = 2$ spectrum is magnified by a factor of 16. Because of an uncertainty in the frequency calibration, the $F = 2$ measurement was stretched by 2% in accordance with the frequency mismatch observed in comparable measurements.

excited states. The residual six observed lines coincide with the predicted bound state energies within 10%. Even stronger evidence for those resonances originating from the hyperfine mixing in the $25P_{3/2}$, $F = 1$ potential curve arises from the direct comparison of both spectra (Fig. 3). Except for the line close to −200 MHz, it is possible to attribute each line in the $F = 2$ spectrum to a corresponding line in the $F = 1$ spectrum. This not only provides strong evidence for the discussed hyperfine mixing, but also allows us to identify which peaks in the $F = 1$ spectrum belong to the mixed potential and which, by exclusion, belong to the triplet potential. The comparable magnitude of the three interactions which couple the different angular momenta [Fig. 1(b)] leads to the before mentioned entanglement between the orbital degree of freedom of the Rydberg electron and the nuclear spin of the ground state atom. Since the interaction between two such molecular entangled states depends on the fine structure state of the Rydberg atom, this can be used to entangle the spin of ground state atoms over the typical length scale of Rydberg-Rydberg interactions.

In contrast to the strong lines in the entanglement regime, it is more challenging to observe the hyperfine mixing in the spin-flip regime. Nevertheless, due to the high signal-to-noise ratio provided by the ion signal, we are able to see a molecular line at −14.8 GHz in the $F = 2$ spectrum [Fig. 2(e)], which, in comparison with the calculated PECs, can only be attributed to the $25P_{1/2}$, $F = 1$ state [highlighted region in Fig. 2(b)]. Since the observed line differs only by 32 MHz from the expected energy of the lowest bound state in the well at 692 a_0 of the $25P_{1/2}$, $F = 1$ mixed potential, we assume the admixture of the $F = 2$ state to be on the order of $\epsilon^2 = 0.04\%$. The detection of bound states at higher internuclear distances is hindered by the small hyperfine mixing. At closer distances, on the other hand, the reduced probability of finding a pair of atoms decreases and pushes the line strength below our detection limit. It should be noted that the observed molecular line has the lowest energy of all possible transitions depicted in Fig. 1, and thus, the presence of $F = 1$ atoms in the initial sample can not explain the observed signal. Thus, we have experimentally shown a spin flip of the ground state perturber upon photoassociation of a Rydberg molecule over a distance of 35 nm between the two atoms.

Because of the high particle density and the presence of collective modes in the BEC, many-body effects beyond the two-particle picture might influence the observed spin-flip mechanism. However, the possibility for spectroscopically addressing a well-defined molecular state allows us to selectively photoassociate only atom pairs that do not have any additional ground state atom inside the Rydberg wave function. Furthermore, bound states of two or more perturber atoms [39] are strongly suppressed due to the geometric constraints imposed by the p-state wave function [34]. Also, the molecular formation process can hardly excite collective modes in the BEC [40,41] as the size of the molecules is much smaller than the healing length $\xi = 230$ nm.

When the separation between the two atoms in the molecular state is much smaller than the typical interparticle distance in a quantum gas or in an optical lattice, the resulting interaction might still be classified as "short-range." It can then be used to modify the contact interaction between the atoms. In fact, optical Feshbach resonances are based on the coupling of a free two-particle scattering state to a molecular bound state with a photoassociation laser. Because of intrinsic losses, molecular states with long lifetimes and minimal off-resonant scattering from the bare atomic resonance are mandatory to apply this concept. Experiments have, so far, been performed on different atomic species, most promising results have been obtained for ytterbium and strontium [30]. The latter features a molecular decay rate of $\gamma/2\pi = 14$ kHz [30]. While a shift in the scattering length could be demonstrated successfully, losses still pose a serious challenge. With the presented spin-flip mechanism, Rydberg molecules can overcome these limitations, due to the absence of scattering from a bare atomic resonance. Furthermore, since the decay rates of $\gamma/2\pi \approx 30$ kHz [extracted from an analysis of the temporal decay in the TOF spectra presented in Fig. 2(b) and in agreement with the natural lifetime of the $25P$ state] are compatible, we speculate that the coupling to spin-flipped Rydberg molecules is, in principle, suited to implement optical Feshbach resonances without scattering from a nearby bare atomic resonance.

For the resonant excitation of Rydberg molecules, nonunitary time evolution occurs. Upon excitation, spontaneous decay of the Rydberg molecules and associative ionization [37] lead to the loss of one or both atoms. However, these losses occur only for the addressed combination of hyperfine states [Fig. 1(c)]. Therefore, in an optical lattice with a two component quantum gas, one could induce losses in doubly occupied sites with a specific spin composition. The phase space dynamics can then drive the system in a correlated spin state, which is decoupled from the loss process.

In conclusion, we have performed high resolution photoassociation spectroscopy of p-state Rydberg molecules and have demonstrated spin-flip collisions in Rydberg molecules. In our case, these spin-flip processes happen for an interatomic distance of about 35 nm. We also resolve molecular states, which feature strong entanglement between the orbital angular momentum of the Rydberg electron and the nuclear spin of the ground state perturber atom. Our results point at the possible realization of optical Feshbach resonances employing Rydberg molecules and provide new means to induce unitary and nonunitary interactions in ultracold quantum gases. This approach works for all atomic species or mixtures which support Rydberg molecules.

We thank C. Greene and J. Pérez-Ríos for valuable discussions about the spin flip processes and the potential energy curves. We thank C. Lippe for discussing the manuscript and I. Fabrikant for providing the Rb-e^--scattering phase shifts. We acknowledge financial support by the DFG within the SFB/TR49. O. T. is funded by the Graduate School of Excellence MAINZ.

*ott@physik.uni-kl.de

[1] M. Greiner, O. Mandel, T. Esslinger, T. W. Hänsch, and I. Bloch, Nature (London) **415**, 39 (2002).
[2] B. Paredes, A. Widera, V. Murg, O. Mandel, S. Fölling, I. Cirac, G. V. Shlyapnikov, T. W. Hänsch, and I. Bloch, Nature (London) **429**, 277 (2004).
[3] M. J. H. Ku, A. T. Sommer, L. W. Cheuk, and M. W. Zwierlein, Science **335**, 563 (2012).
[4] C. Chin, R. Grimm, P. Julienne, and E. Tiesinga, Rev. Mod. Phys. **82**, 1225 (2010).
[5] M. Olshanii, Phys. Rev. Lett. **81**, 938 (1998).
[6] Z. Hadzibabic and J. Dalibard, Riv. Nuovo Cimento **34**, 389 (2011).
[7] S. Fölling, S. Trotzky, P. Cheinet, M. Feld, R. Saers, A. Widera, T. Müller, and I. Bloch, Nature (London) **448**, 1029 (2007).
[8] K. Baumann, C. Guerlin, F. Brennecke, and T. Esslinger, Nature (London) **464**, 1301 (2010).
[9] A. Griesmaier, J. Werner, S. Hensler, J. Stuhler, and T. Pfau, Phys. Rev. Lett. **94**, 160401 (2005).
[10] M. Lu, N. Q. Burdick, S. H. Youn, and B. L. Lev, Phys. Rev. Lett. **107**, 190401 (2011).
[11] K. Aikawa, A. Frisch, M. Mark, S. Baier, A. Rietzler, R. Grimm, and F. Ferlaino, Phys. Rev. Lett. **108**, 210401 (2012).
[12] K.-K. Ni, S. Ospelkaus, D. J. Nesbitt, J. Ye, and D. S. Jin, Phys. Chem. Chem. Phys. **11**, 9626 (2009).
[13] M. D. Lukin, M. Fleischhauer, R. Côté, L. M. Duan, D. Jaksch, J. I. Cirac, and P. Zoller, Phys. Rev. Lett. **87**, 037901 (2001).
[14] K. Singer, M. Reetz-Lamour, T. Amthor, L. G. Marcassa, and M. Weidemüller, Phys. Rev. Lett. **93**, 163001 (2004).
[15] D. Tong, S. M. Farooqi, J. Stanojevic, S. Krishnan, Y. P. Zhang, R. Côté, E. E. Eyler, and P. L. Gould, Phys. Rev. Lett. **93**, 063001 (2004).
[16] A. Gaëtan, Y. Miroshnychenko, T. Wilk, A. Chotia, M. Viteau, D. Comparat, P. Pillet, A. Browaeys, and P. Grangier, Nat. Phys. **5**, 115 (2009).
[17] T. Amthor, C. Giese, C. S. Hofmann, and M. Weidemüller, Phys. Rev. Lett. **104**, 013001 (2010).
[18] T. Weber, M. Höning, T. Niederprüm, T. Manthey, O. Thomas, V. Guarrera, M. Fleischhauer, G. Barontini, and H. Ott, Nat. Phys. **11**, 157 (2015).
[19] P. Schauß, M. Cheneau, M. Endres, T. Fukuhara, S. Hild, A. Omran, T. Pohl, C. Groß, S. Kuhr, and I. Bloch, Nature (London) **491**, 87 (2012).
[20] J. Zeiher, R. van Bijnen, P. Schau, S. Hild, J. yoon Choi, T. Pohl, I. Bloch, and C. Groß, arXiv:1602.06313 [Nat. Phys.].
[21] J. E. Johnson and S. L. Rolston, Phys. Rev. A **82**, 033412 (2010).
[22] C. Boisseau, I. Simbotin, and R. Côté, Phys. Rev. Lett. **88**, 133004 (2002).
[23] K. R. Overstreet, A. Schwettmann, J. Tallant, D. Booth, and J. P. Shaffer, Nat. Phys. **5**, 581 (2009).
[24] V. Bendkowsky, B. Butscher, J. Nipper, J. P. Shaffer, R. Löw, and T. Pfau, Nature (London) **458**, 1005 (2009).
[25] C. H. Greene, A. S. Dickinson, and H. R. Sadeghpour, Phys. Rev. Lett. **85**, 2458 (2000).
[26] D. Booth, S. T. Rittenhouse, J. Yang, H. R. Sadeghpour, and J. P. Shaffer, Science **348**, 99 (2015).
[27] M. I. Chibisov, A. A. Khuskivadze, and I. I. Fabrikant, J. Phys. B **35**, L193 (2002).
[28] E. L. Hamilton, C. H. Greene, and H. R. Sadeghpour, J. Phys. B **35**, L199 (2002).
[29] T. Niederprüm, O. Thomas, T. Eichert, C. Lippe, J. Pérez-Ríos, C. H. Greene, and H. Ott, Nat. Commun. **7**, 12820 (2016).
[30] T. L. Nicholson, S. Blatt, B. J. Bloom, J. R. Williams, J. W. Thomsen, J. Ye, and P. S. Julienne, Phys. Rev. A **92**, 022709 (2015).
[31] E. Fermi, Nuovo Cimento **11**, 157 (1934).
[32] A. Omont, J. Phys. (Paris) **38**, 1343 (1977).
[33] D. A. Anderson, S. A. Miller, and G. Raithel, Phys. Rev A **90**, 062518 (2014).
[34] H. Saßmannshausen, F. Merkt, and J. Deiglmayr, Phys. Rev. Lett. **114**, 133201 (2015).
[35] F. Böttcher, A. Gaj, K. M. Westphal, M. Schlagmüller, K. S. Kleinbach, R. Löw, T. C. Liebisch, T. Pfau, and S. Hofferberth, Phys. Rev. A **93**, 032512 (2016).
[36] T. Manthey, T. M. Weber, T. Niederprüm, P. Langer, V. Guarrera, G. Barontini, and H. Ott, New J. Phys. **16**, 083034 (2014).

[37] T. Niederprüm, O. Thomas, T. Manthey, T. M. Weber, and H. Ott, Phys. Rev. Lett. **115**, 013003 (2015).

[38] M. Schlagmüller, T. C. Liebisch, F. Engel, K. S. Kleinbach, F. Böttcher, U. Hermann, K. M. Westphal, A. Gaj, R. Löw, S. Hofferberth, T. Pfau, J. Pérez-Ríos, and C. H. Greene, Phys. Rev. X **6**, 031020 (2016).

[39] A. Gaj, A. T. Krupp, J. B. Balewski, R. Löw, S. Hofferberth, and T. Pfau, Nat. Commun. **5**, 4546 (2014).

[40] T. Karpiuk, M. Brewczyk, K. Rzążewski, A. Gaj, J. B. Balewski, A. T. Krupp, M. Schlagmüller, R. Löw, S. Hofferberth, and T. Pfau, New J. Phys. **17**, 053046 (2015).

[41] J. Wang, M. Gacesa, and R. Côté, Phys. Rev. Lett. **114**, 243003 (2015).